



Calibration Services, Inc.
47 W. 66th St.
New York, NY 10023

To: Laura Jones, Chief Technical Officer
HVAC Services Corp.
5312 Ashtabula Road.
Traverse City, MI 49684

From: Jack McGregor, Omer Khan, Luis Barcenas, Landon Harris
G.G. Brown Building, 2350 Hayward St,
Ann Arbor, MI 48109

Subject: Calibration of load, pressure, and temperature instrumentation for E-Corporation

Date: October 30, 2024

Distr: Evaluation of R-134a food storage unit

FOREWORD

Ecochill is creating an efficient solar powered refrigeration system as an eco-friendly option for remote communities and off-grid applications. This requires strong commitment to sustainability and reliability while maintaining adequate performance. To see if a lower cost, adequately performing option is possible, you have provided a Hampden H-CRT-1 trainer cart with R-134a refrigerant and mounted temperature, pressure and mass flow sensors for testing. You have asked us to provide temperature-specific entropy (T-s) diagrams of the unit with heat exchange to and from the ambient air with the condenser and evaporator at 100% speed. Additionally, we are to provide this for three separate operating angular speeds for the compressor at 45, 50 and 59 Hz. You also asked us to report the cooling capacity, coefficient of performance (CoP), and power demanded by the compressor for each angular speed. To conclude, you asked us to evaluate the system feasibility and possible cost saving with the condition of running the compressor below 59 Hz speed without compromising performance. We have included all errors associated with resolution, accuracy, and precision in our calculations and results.

SUMMARY

We evaluated the performance of the Hampden H-CRT-1 test cart with the compressor set to three different angular speeds: 45, 50 and 59 Hz. As requested we have created temperature-specific entropy (T-s) diagrams for the unit with heat exchange to and from the ambient air with the condenser and evaporator at 100% speed. We also found that decreasing the compressor speed would not significantly change the cooling capacity but increase the coefficient of performance due to lower thermodynamic power input, and cause decreased power demand for the compressor. As solar panel costs increase with higher power ratings, we found that decreasing the compressor speed would reduce up-front costs for the refrigeration system. This, along with the coefficient of performance increasing with lower compressor speeds, leads us to recommend running the compressor at the lowest speed possible, which in our case was 45 Hz.

METHODS

This section illustrates the process followed to obtain data for the vapor compression cycle created by the Hampden H-CRT-1 under different compressor speeds, as well as how we determined the cooling capacity of the system, coefficient of performance, and the power demand for the compressor for each of our three trials. [1][6]

Vapor Compression Cycle

We simulated the Vapor Compression Cycle, the cycle used in refrigeration, using the provided Hampden H-CRT-1. We started the cycle by turning on the fans for the condenser and evaporator #1 to operate at full speed and specifying the compressor speed. We tested 3 compressor speeds: 45 Hz, 50 Hz, and 59 Hz. We were not able to measure a compressor speed of 60 Hz as requested because the maximum compressor speed of the H-CRT-1 was 59 Hz, but we believe this will be sufficient as it is much closer to 60 Hz than the other tested speeds and we will be able to see differences in any measured or calculated values due to decreased compressor speed if they exist. We then waited for the cycle to reach its steady state, which we confirmed by seeing when the analog Brooks GT1350 Sho-Rate G rotameter gave a constant flow rate reading. Once the cycle reached steady state, we used the provided LabView program to take and record temperature, pressure, and power measurements at the input and output of the evaporator, expansion valve (throttle), condenser, and compressor. We used an Omega Engineering TT-T-20-SLE for all temperature readings, a Cole Parmer 07356-53 for the pressure readings at the input and output of the evaporator and the output of the condenser, and a Cole Parmer 07356-54 for the pressure readings at the input of the compressor and the output of the condenser. Figure 1 shows the test setup, with the evaporator, expansion valve, condenser, compressor, and two important analog sensors: the pressure gauge and the rotameter, which we measured manually for each trial.

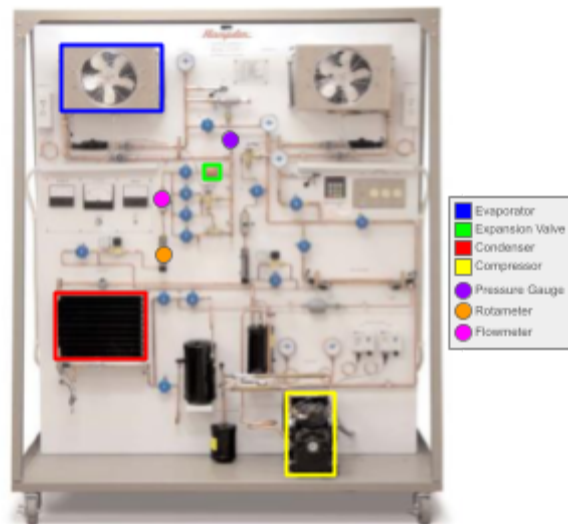


Figure 1. Diagram of the Hampden H-CRT-1 test system outlining the evaporator, expansion valve, condenser, compressor, as well as the analog pressure gauge and rotameter that were measured for each state.

The Vapor Compression Cycle that was tested with the refrigeration systems follows a diagram that is represented in Figure 2. The T-s diagram further outlines Figure 1 by mapping the fluid's thermodynamic states throughout its cycle. Points 1 through 4 on the diagram correspond to the thermodynamic state in the stages of the refrigeration cycle. Point 1a represents the refrigerant leaving the evaporator and point 1b represents the refrigerant entering the compressor from the cold reservoir as a vapor, through thermodynamic power. Point 2a represents the refrigerant

leaving the compressor in a high temperature and high pressure superheated vapor, and point 2b represents the refrigerant entering the condenser. Point 3 represents the refrigerant leaving the condenser after losing heat, where it condensed into a saturated liquid and enters the expansion, or throttle, valve. Point 4 represents the fluid after exiting the expansion valve, where the fluid is a two phase mixture and drops pressure, then enters the evaporator and reaches a low temperature and low pressure fluid and evaporates as temperature and pressure are constant. The values for specific enthalpy, s , as well as specific entropy, h , for R-134a at each of these points were found by entering the measured temperature and pressure in a thermodynamic data program called CAT31 [4].

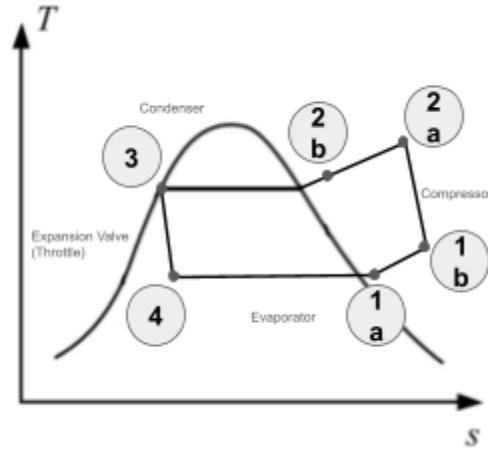


Figure 2. General T-s diagram for a vapor compression refrigeration cycle[11][12] with labeled states that correspond to temperature or pressure sensor locations.

Although most measurements were taken automatically and recorded in LabView, we had to take some measurements manually using the analog devices placed on the H-CRT-1. One of these measurements was the gauge pressure at point 4 for each of the three trials, right before the liquid R-134a enters the evaporator, using a Yellow Jacket 49056 pressure gauge. We added this gauge pressure to the measured atmospheric pressure of the lab room by a Meade TE866-W, $0.0977 \pm 5 \times 10^{-5}$ MPa, to get the total pressure used in calculations. The other manual measurement we took was the reading of the Brooks GT1350 Sho-Rate G rotameter for each trial, which was placed at point 3, right after the refrigerant has gone through the condenser and is in a saturated liquid phase. We used this reading and the table in reference chart [8] to obtain a volumetric flow rate of R-134a, and we then used the measured temperature of the condenser output from LabView and the table in reference chart [9] to obtain the density of the refrigerant (assuming the output of the condenser is entirely saturated liquid). Multiplying these two values gave us the mass flow rate of R-134a for each trial, which remains constant throughout the cycle. These values are shown in Table 1 below.

Table 1. Values obtained through analog measurements in the H-CRT1.

Compressor Speed	Gauge Pressure at Point 4 (MPa)	Volumetric Flow Rate (m^3/s)	R-134a Density (kg/m^3)	Mass Flow Rate (kg/s)
45 Hz	0.27 ± 0.03	$6.3 \times 10^{-6} \pm 9 \times 10^{-8}$	$1.17 \times 10^3 \pm 1$	$7.4 \times 10^{-3} \pm 1 \times 10^{-4}$
50 Hz	0.28 ± 0.03	$6.5 \times 10^{-6} \pm 9 \times 10^{-8}$	$1.16 \times 10^3 \pm 1$	$7.6 \times 10^{-3} \pm 1 \times 10^{-4}$
59 Hz	0.24 ± 0.03	$6.1 \times 10^{-6} \pm 9 \times 10^{-8}$	$1.16 \times 10^3 \pm 1$	$7.1 \times 10^{-3} \pm 1 \times 10^{-4}$

Cooling Capacity

The cooling capacity in Watts, \dot{Q}_e , of the cycle is a measure of the “energy benefit”, the heat flux taken out of the cool space of the refrigeration system. This was calculated using Equation 1 below [7].

$$\dot{Q}_e = \dot{m}(h_1 - h_4) \quad (1)$$

In Equation 1, \dot{m} is the measured mass flow rate in kg/s and h_1 and h_4 are the specific enthalpies from the CAT31 software in J/kg for point 1 and point 4 of the cycle, respectively. We chose to use the specific enthalpy at point 1a instead of 1b to calculate the cooling capacity because the heat flux is taken out using the evaporator, and point 1a recorded the temperature and pressure right after the refrigerant leaves the evaporator.

Coefficient of Performance

The coefficient of performance [5] is a unitless measure of the performance of the system. It is calculated by dividing the “energy benefit” of the system, the cooling capacity, by the “energy cost” of the system, the thermodynamic power input to the system by the compressor. The cooling capacity is calculated using Equation 1 above, and the thermodynamic power input in Watts, \dot{w}_{comp} , is calculated using Equation 2 below.

$$\dot{w}_{comp} = \dot{m}(h_2 - h_1) \quad (2)$$

In Equation 2, \dot{m} is the measured mass flow rate in kg/s and h_2 and h_1 are the specific enthalpies from the CAT31[4] software in J/kg for point 2 and point 1 of the cycle, respectively. We chose to use the specific enthalpy at point 2a instead of 2b to calculate the power input as the power input comes from the compressor, and point 2a recorded the temperature and pressure right after the refrigerant leaves the compressor, and we chose to use the specific enthalpy at point 1a instead of 1b to calculate the power input to account for any power needed to overcome losses due to the accumulator between the evaporator and compressor.

With the cooling capacity and thermodynamic power inputs calculated, we divided the cooling capacity by the thermodynamic power input to obtain the coefficient of performance for each trial.

Power Demand for Compressor

The power demand for the entire H-CRT-1 system was measured with a Yokogawa PR300 Power Energy Meter[10] and recorded in LabView. This power demand will be higher than the thermodynamic power input to the system because no thermodynamic cycle is 100% efficient and will be higher than the actual power demanded by the compressor as we are measuring the power used to run all devices in the system, not only the compressor. The power demanded by the compressor will be between the calculated thermodynamic output of the system and the measured power demand for the entire system, and we can assume a trend in the power demanded by the compressor if the other two pressures follow similar trends.

RESULTS

This section presents T-s diagrams for the three trials performed at different compressor speeds, the final results for the cooling capacity and coefficient of performance of the system for these trials, as well as an estimation for the power demanded by the compressor for these trials.

System Performance

Using the measured temperatures from the thermocouples at the six points defined in Figure 2 and the specific entropies for these points given by the CAT31 program, we were able to plot T-s curves for the three tested compressor speeds as shown in Figure 3 below.

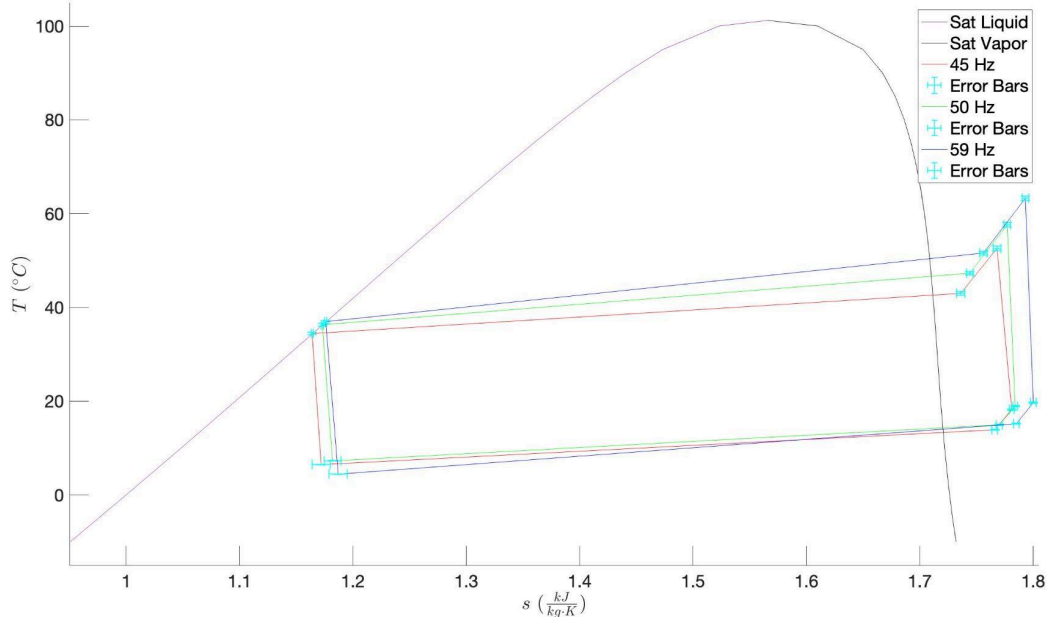


Figure 3. T-s diagrams for the H-CRT-1 vapor compression cycle at three different compressor speeds with error bars. In the foreground is the R-134a vapor dome to illustrate where our states lie in reference to it.

Cooling Capacity

The specific enthalpies at point 1a and 4 from the CAT31 program, as well as the cooling capacities calculated using Equation 1, for the three trials are shown in Table 2 below. We found that the specific enthalpies for points 1a and 4 are extremely similar for all three trials, increasing slightly as compressor speed increases. This gave us similar cooling capacities for the three trials, lying between 1.14 ± 0.02 kW and 1.22 ± 0.02 kW. The cooling capacity increases slightly from 45 Hz to 50 Hz then decreases more from 50 Hz to 59 Hz, which comes from the mass flow rates following the same trend (as seen in Table 1). The low error, caused mostly by accuracy error in the pressure measurements, give us confidence the cooling capacities are correct.

Table 2. Specific enthalpy at points 1a and 4, as well as the calculated cooling capacities for each trial.

Compressor Speed	Specific Enthalpy at Point 1a (kJ/kg)	Specific Enthalpy at Point 4 (kJ/kg)	Cooling Capacity (kW)
45 Hz	410.6 ± 0.2	248.1 ± 0.4	1.20 ± 0.02
50 Hz	411.6 ± 0.4	250.9 ± 0.4	1.22 ± 0.02
59 Hz	412.7 ± 0.2	251.9 ± 0.4	1.14 ± 0.02

Coefficient of Performance

The specific enthalpies at point 2a and 1a from the CAT31 program, the thermodynamic power input calculated using Equation 2, and the calculated coefficients of performance for the three trials are shown in Table 3 below. We found that the specific enthalpies increase with increasing compressor speed at point 2a, while increasing at a lower rate at point 1a. This led to the thermodynamic power input increasing with compressor speed, which led to higher coefficients of performance for the trials with lower compression speed. The low error in thermodynamic

power input, caused mostly by higher error in the specific enthalpies at point 2a, give us confidence that the thermodynamic power inputs and coefficients of performance are correct.

Table 3. Specific enthalpy at points 2a and 1a, the calculated thermodynamic power input, as well as the calculated coefficient of performance for each trial.

Compressor Speed	Specific Enthalpy at Point 2a (kJ/kg)	Specific Enthalpy at Point 1a (kJ/kg)	Thermodynamic Power Input (W)	Coefficient of Performance
45 Hz	435.3 ± 0.6	410.6 ± 0.2	183 ± 5	6.6 ± 0.2
50 Hz	439.6 ± 0.6	411.6 ± 0.4	212 ± 6	5.8 ± 0.2
59 Hz	445.3 ± 0.6	412.7 ± 0.2	232 ± 6	5.0 ± 0.1

Power Demand for Compressor

The measured power demand of the system from LabView for each trial is shown in Table 4 below. We found that the power demand increases with increasing compressor speed. The low errors, caused mostly by precision errors in the power measurements, give us confidence that the power demands are accurate.

Table 4. Measured power demand of the system for each trial.

Compressor Speed	Power Demand (W)
45 Hz	383.2 ± 0.1
50 Hz	408.2 ± 0.2
59 Hz	444.8 ± 0.2

Although we could not directly measure the power demanded by the compressor at each speed setting, we know it will lie between the calculated thermodynamic power input in Table 3 and the power demanded by the entire system in Table 4. Since these two powers increase with increased compressor speed, we can conclude that the power demanded by the compressor will also increase with increased compressor speed.

DISCUSSION

We found that the power demand, both for the compressor and the entire system, increases with increasing compressor speed. In the case of the solar panels used in your products, a higher power demand leads to higher cost. This means that using lower compressor speeds will lead to lower up-front costs as you can purchase solar panels with lower power ratings. We also found that lowering the compressor speed leads to higher coefficients of performance, meaning that lowering the compressor speed will lead to improved performance rather than compromised performance.

CONCLUSIONS AND RECOMMENDATIONS

For the application of the solar powered refrigeration system, we were asked to assess whether reducing compressor speed would be feasible and decrease the up-front cost of the system without compromising system performance. We found that decreasing the compressor speed would not affect the cooling capacity greatly and decrease the thermodynamic power input to the system, leading to a higher coefficient of performance. We also found that the compressor would demand less power for lower compressor speed. This means that decreasing the compressor speed would decrease the up-front cost of the system, as solar panels with higher power ratings cost more, and improve the performance of the system. Because of this, we recommend you run the compressor at a speed lower than 59 Hz. We recommend the lowest speed possible, which for our tests was 45 Hz, as this will lead to the lowest cost and best performance.

REFERENCES

- [1]Araner. (n.d.). *Vapor compression system: Compression cycle*. ARANER.
<https://www.araner.com/blog/vapor-compression-refrigeration-cycle#:~:text=The%20Vapor%20Compression%20Refrigeration%20Cycle%20involves%20four%20components%3A%20compressor%2C%20condenser,it%20flows%20from%20an%20evaporator.>
- [2]Blundell, S., & Blundell, K. M. (2019). *Concepts in thermal physics*. Oxford University Press.
- [3]Borgnakke, C., & Sonntag, R. E. (2014). *Fundamentals of thermodynamics*. Wiley.
- [4]*Catt: Computer-aided thermodynamic tables*. WorldCat.org. (n.d.).
<https://search.worldcat.org/nl/title/CATT:-computer-aided-thermodynamic-tables/oclc/503519466>
- [5]*Coefficient of performance*. Coefficient of Performance - an overview | ScienceDirect Topics. (n.d.).
<https://www.sciencedirect.com/topics/engineering/coefficient-of-performance>
- [6]*How does a compression refrigeration system work?*. Process Solutions, Inc. (2024, July 2). <https://processsolutions.com/how-does-a-compression-refrigeration-system-work/>
- [7]Evans, P. (2021, February 14). *Chiller cooling capacity - how to calculate*. The Engineering Mindset.
<https://theengineeringmindset.com/chiller-cooling-capacity-calculate/>
- [8]*M canvas login*. U. (n.d.).
https://umich.instructure.com/courses/700167/files/36543521?module_item_id=3995851
- [9]*Schaum's outline of thermodynamics for Engineers, third edition*. (2014). . McGraw-Hill Professional.
- Note for [9]: The actual flow meter conversion sheet could not be found online.
- [10]Wordpress. (n.d.).
<https://heatingairconditioningfundamentals.wordpress.com/wp-content/uploads/2018/04/hamphen-operating-instruction.pdf>
- [11]Uobasrah. (n.d.-a). <https://faculty.uobasrah.edu.iq/uploads/teaching/1688286290.pdf>
- [12]Design of vapor-compressionrefrigeration cycles. Design of Vapor-Compression Refrigeration Cycles. (n.d.).
<https://www.qrg.northwestern.edu/thermo/design-library/refrig/refrig.html>